Electronic Supplementary Material (ESI) for Nanoscale.
This journal is © The Royal Society of Chemistry 2017

Supporting Information

"Installation art"-like hierarchical self-assembly of giant polymeric elliptic platelets

Lei Huang,[a] Zuotao Lei,[a] Tong Huang,[b] Yongfeng Zhou,[b] Yongping Bai[a*]*

[a]*School of Chemistry and Chemical Engineering, Harbin Institute of Technology, Harbin 150001, P.R. China. Email: baifengbai@hit.edu.cn*
[b]*School of Chemistry and Chemical Engineering, State Key Laboratory of Metal Matrix Composite, Shanghai Jiao Tong University, Shanghai 200240, China. Fax: (+86) 21 54741297; Email: yfzhou@sjtu.edu.cn*

1. Materials.

1,4-Bis (3-aminopropyl) piperazine (TCI, >98%), α,ω-Dicarboxyl Poly (Ethylene Glycol) (Aldrich, average Mn = 600 and 250) and sodium hypophosphite (Sigma-Aldrich, >99%) were used as received.

2. Instruments and Measurements

Fourier Transform Infrared Spectroscopy (FTIR)

FTIR measurement was carried out on a Perkin-Elmer Spectrum 100 PC Fourier transform infrared spectrometer in the range of 500~4500 cm^{-1} with an accuracy of 4 cm^{-1}.

Nuclear Magnetic Resonance (NMR)

The Varian Mercury Plus spectrometer was used to obtain ^1H NMR spectra (400 MHz) with sulfuric acid (DMSO-d_6) used as solvent.

Gel Permeation Chromatography (GPC)

GPC measurement was carried out via an HLC-8320GPC system at 40^oC with THF as mobile phase at a flow rate of 0.6 mL/min.

Scanning Electron Microscope (SEM)

Scanning electron microscopy analysis was performed on a NOVA NanoSEM 450 (PEI). The samples for SEM test were prepared by depositing several drops of the self-assembly solution onto the surface of cleaned silicon wafer and air-dried at room temperature. The samples were coated with a thin film of gold or platinum before measurement.

Atomic Force Microscopy (AFM)

AFM measurements were carried out on a multimode Nanoscope-IIIa Scanning Probe Microscope equipped with a MikroMasch silicon cantilever, NSCII (radius < 10nm, resonance frequency = 300kHz, spring constant = 40N/m) with tapping mode (TM) at room temperature. The sample for AFM observations were prepared by depositing several drops of the solution onto the surface of fresh cleaved mica, and the samples were air-dried at room temperature.

Wide-Angle X-Ray Diffraction (WXRD)

WAXD patterns was performed on a Bruker Dalton D8 Advance spectrometer with Cu K_α radiation (λ = 1.541 Å), and the scanning rate was 2^o per minute from 5^o to 30^o (2θ). The q vector values were calculated according to the equation: $q = 4\pi\sin\theta/\lambda$. The powder samples for WXRD test were prepared by freeze-dried of the self-assembly dispersion in vacuum.

Small-Angle X-Ray Scattering (SAXS)

The SAXS measurements were carried out using a SAXSess mc2 apparatus, which used a Cu K_α radiation source. The wave vector (q) was determined by $q = 4\pi\sin\theta/\lambda$, where 2θ is the scattering angle, and λ is the wavelength. According to the equation: $d = 2\pi/q$, the length of periodic structures in the prepared self-assembly can be obtained.

2. Synthesis and Characterization of PAPIP.26

The polyamide, PAPIP.26, was synthesized by forming-salts and solution-melt polycondensation following the reaction method described by our previous work.[1-3] As show in Scheme 1a, α,ω-Dicarboxyl Poly (Ethylene Glycol) was dissolved in deionized water and added slowly into the aqueous solution of 1,4-Bis (3-aminopropyl) piperazine with vigorously stirring. After 2 h, the pink oil liquid, PAPIP.26 salt, was obtained via rotary evaporation. Then this PAPIP.26 salt was dried in a vacuum oven overnight with a typical temperature of 40 ^{o}C.

Then, the obtained PAPIP.26 salt was dissolved in deionized water. Then the solution was transferred to an autoclave. Then the autoclave was evacuated and flushed with nitrogen for three times. First, the autoclave was heated until 160 ^{o}C. After 30 min, the temperature was increased to 200 ^{o}C. Subsequently, the pressure was gradually decreased to atmospheric pressure in 2 h and the reaction temperature was increased to 250 ^{o}C. Then the autoclave was evacuated for further polycondensation. Three hours later, the reaction was stopped and the brown product of PAPIP.26 was obtained.

FTIR and ^{1}H NMR were used to ascertain the structure of as-prepared PAPIP.26. Fig. S1a displays the typical FTIR spectrum of the product, which exhibits the characteristic bands associated with polyamides. Bands with maximums at 3369 cm^{-1} (hydrogen-bonded N-H stretching), round 1655 cm^{-1} (C=O stretching), and round 1540 cm^{-1} (C-N stretching and CO-N-H bending) are all correspond to motions associated with the amide group. The results above can prove the formation of polyamide. Fig. S1b shows the ^{1}H NMR spectrum of the prepared PAPIP.26 along with the peak assignments in dimethyl sulfoxide-d_6. The resonance peaks appearing in the region of 7.70 ppm in the spectrum also support the formation of amide linkages (peak 3). In addition, the chemical shifts at 3.51ppm (peak 2) is attributed to the protons in the methylene groups of the repeat units of α,ω-Dicarboxyl Poly (Ethylene Glycol). The signals at about 3.83 ppm (peak 1) and 3.09 ppm (peak 4) stem from the protons adjacent to the amide groups. Furthermore, the peak at 2.31 ppm (peak 6) comes from the protons adjacent the piperazine ring. And the resonance of the piperazine ring (peak 7) is at 2.24 ppm. The chemical shifts at 1.54 ppm (peak 5) is assigned to the other protons in the methylene moiety.

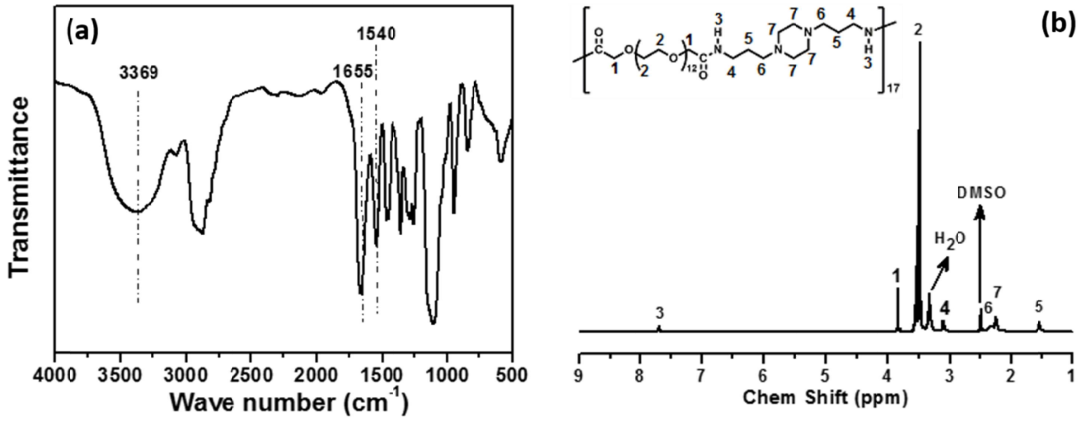

Fig. S1 The FTIR and ^{1}H NMR spectra of as-prepared PAPIP.26.

3. The GPC measurement of PAPIP.26

The GPC measurements (Fig. S2) showed a distribution with a number-average molecular weight of 13 KDa and a polydispersity of 2.8.

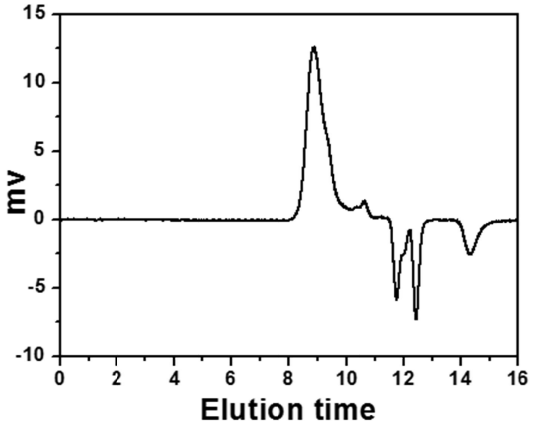

Fig. S2 The GPC traces of PAPIP.26 with dimethyl formamide (DMF) as eluent.

4. The SEM and AFM images of elliptic superstructures

The SEM images (Fig. S3a) demonstrate the aggregates are polydisperse elliptic structures. In addition, the largest elliptic platelet possess more than 60 μm axial length, which is close to the diameter of people's hair (Fig. S3b). The AFM images (Fig. S3c and S3d) further ascertain the elliptic structure of the PAPIP.26 self-assemblies. According to the height profiles of the elliptic self-assemblies (Inset in Fig. S3d), we can conclude that the average axial length of the self-assemblies is more than 20 μm. Furthermore, these elliptic structure have a relatively flat surface, which further support the morphology of elliptic platelets (Fig. 1).

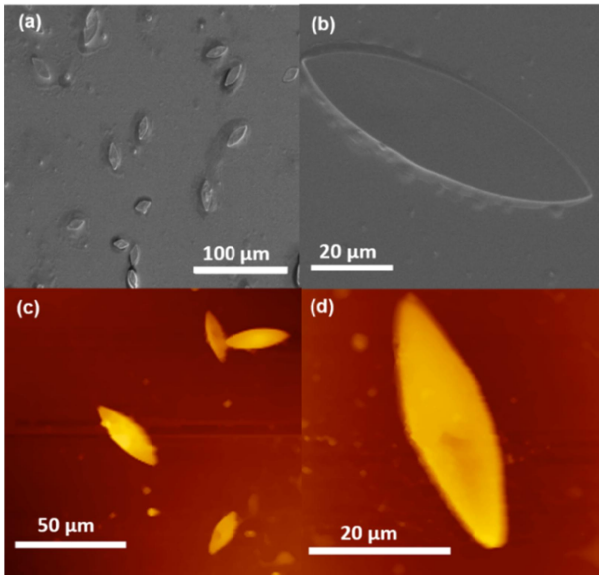

Fig. S3 The SEM (a, b) and AFM (c, d) images of PAPIP.26 self-assemblies in aqueous solution with the concentration of 0.6 mg/mL.

5. Characterizations of the PAPIP.26 self-assemblies in dilute aqueous solution

AFM was used to characterize the morphology of the self-assemblies from PAPIP.26 at the concentration of 0.05 mg/mL. Fig. S4 displays the typical AFM height image and height profiles of the shape-asymmetric particles of PAPIP.26. From Fig. S4a and S4b, a large number of polydisperse noncentrosymmetric particles with well-defined geometric shape (a quadrangular frustum pyramid shape) and sharp edges could be observed. And the height profiles mean that these particles have shown a relatively flat surface.

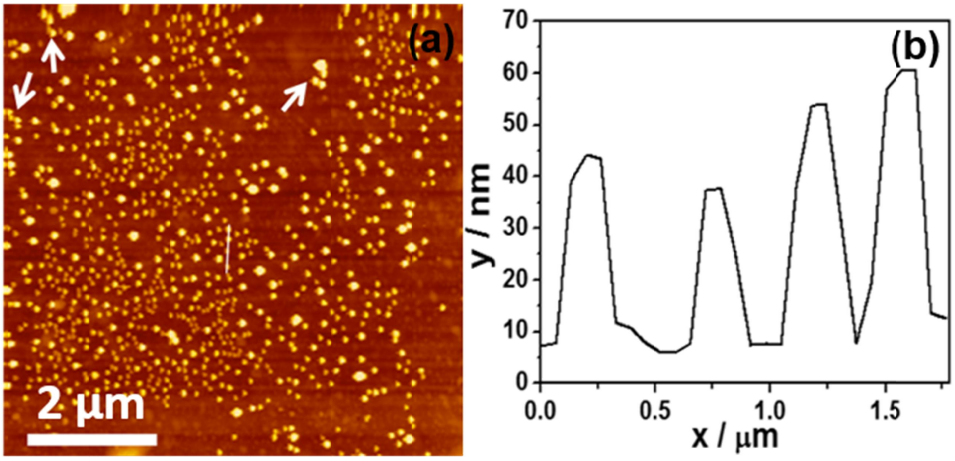

Fig. S4 The AFM height image (a) and height profiles (b) of the self-assemblies from PAPIP.26 at the concentration of 0.05 mg/mL.

6. Characterization of the intermediate of elliptic platelet structure

Fig. S5 shows some elliptic platelet intermediates from which a multilayer structure for the platelet could be seen clearly according to the defects. In addition, the building blocks of small platelets could also be discerned inside the giant platelet.

From Fig. S6, we can observe that some particles have not yet fused and stack together in the inner and surface of elliptic platelet structure. And what's more, several layer can be seen and have not yet fused.

Form both Fig. S5 and S6, it could also be concluded that the giant platelets were formed thorough the fusion of the small building blocks inside. Thus, the smooth giant platelets as shown in Fig. 1 in main text were finally obtained.

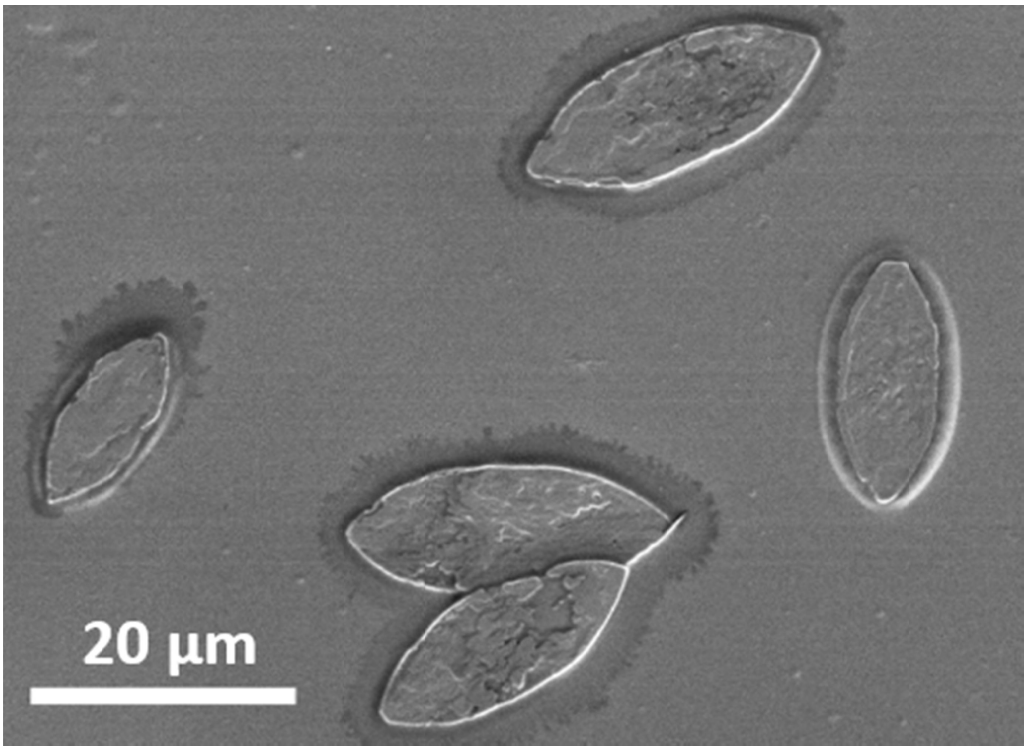

Fig. S5 The SEM image of the intermediate of the obtained elliptic platelet-like structure (c = 0.6 mg/mL).

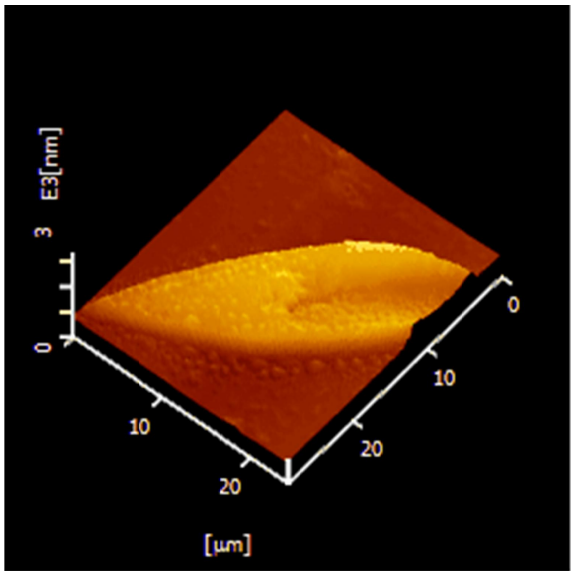

Fig. S6 The AFM 3D image of the intermediate of the obtained elliptic platelet-like structure (c = 0.6 mg/mL).

7. The installation art

Fig. S7 A photograph showing some examples of the installation art. The platelet objects with regular geometric shapes in the image were installed from the small wooden chips.

8. Calculation of the molecular length of repeat units in polyamide molecule

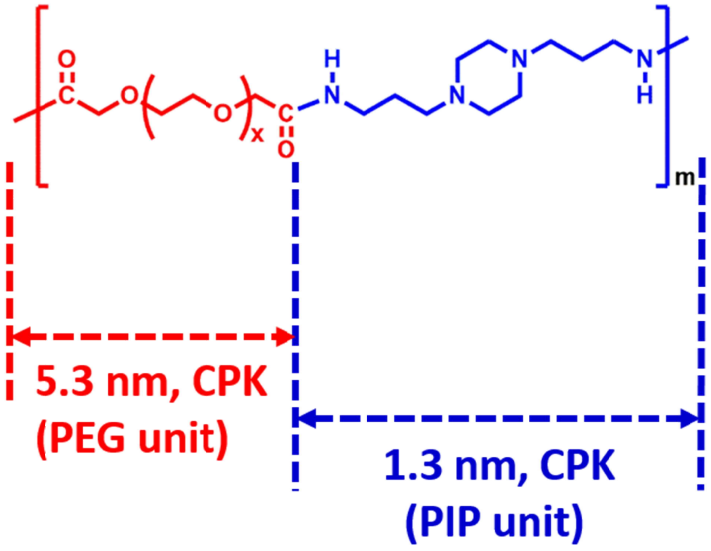

Fig. S8 Estimating the length of repeat units in an extended polyamide molecule according the CPK model. The extended length of PEG unit is 5.3 nm, which agrees well with the SAXS data (Fig. 3c). The extended length of PIP unit is 1.3 nm; however, it is 0.64 nm in length in the giant platelets according to the WXRD pattern (Fig. 3a), which indicates that the PIP segments should pack together with a tilting angle.

9. The morphology of the prepared PAPIP.9 in water

For comparison, we also synthesized another polyamide by the polycondensation of α,ω-dicarboxyl poly (ethylene glycol) (Mn = 250) and 1,4-Bis (3-aminopropyl) piperazine. We denoted it as PAPIP.9. From Fig. S9, we can observe that the prepared PAPIP.9 can self-assemble into spherical nanoparticles.

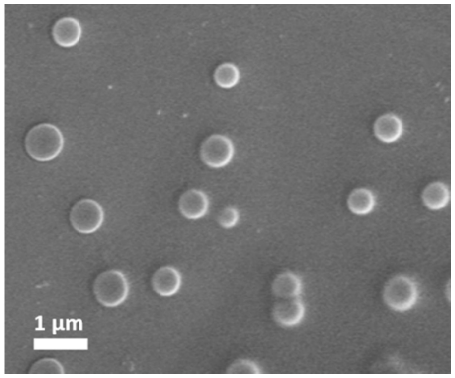

Fig. S9 The SEM image of PAPIP.9 self-assemblies in water.

10. The self-assembly morphologies of PAPIP.26 in THF and DMSO

For comparison, we also investigated the self-assembly behaviors of PAPIP.26 in DMSO and THF, respectively. From Fig. S10a, we can observe that PAPIP.26 can not self-assemble into well-defined structure in THF. On the contrary, when the concentration of the PAPIP.26 in DMSO is 0.06 mg/mL, we can observe that PAPIP.26 can self-assemble into spherical particles covered with small particles on the surface and with an average size of 1 μm from Fig. S10b. When more PAPIP.26s were added into the solution to reach a concentration of 0.6 mg/mL, larger spherical structures with an average diameter of 1.5 μm were obtained according to the SEM image (Fig. S10c), and these spherical structures are covered by some small particles, too. Interestingly, if we further increased the polymer concentration to 1 mg/mL, we can observe some larger spherical particles covered with the crossed lamella, which the average size is about 2.9 μm (Fig. S10d). And what's more, the obtained spherical particles might possess the hollow structures according to the inset image in Fig. S10d. The above morphology transformation might be driven by the crystallization of PAPIP.26.

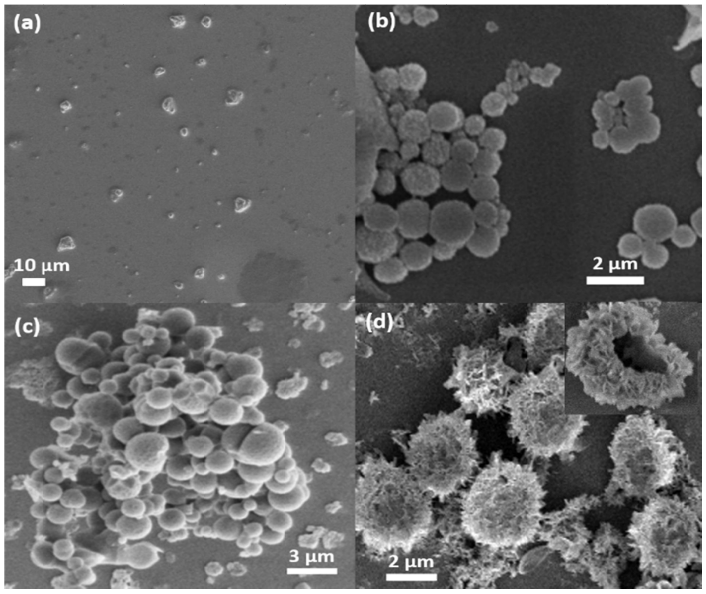

Fig. S10 The SEM images of PAPIP.26 self-assemblies in different solvents. (a) THF; (b) DMSO (c = 0.05 mg/mL); (c) DMSO (c = 0.6 mg/mL); (d) DMSO (c= 1 mg/mL).

References

[1] Li, Y. J.; Yan, D. Y. *Polymer* **2001**, 42, 5055.

[2] Cui, X. W.; Yan, D. Y. *Eur. Polym. J.* **2004**, 40, 1111.

[3] Li, Y. J.; Yan, D. Y.; Zhu, X. Y. *Eur. Polym. J.* **2001**, 37, 1849.